Models of molecular geometry

Ronald J. Gillespie and Edward A. Robinson

Received 20th November 2004
First published as an Advance Article on the web 11th April 2005
DOI: 10.1039/b405359c

Although the structure of almost any molecule can now be obtained by *ab initio* calculations chemists still look for simple answers to the question "What determines the geometry of a given molecule?" For this purpose they make use of various models such as the VSEPR model and qualitative quantum mechanical models such as those based on the valence bond theory. The present state of such models, and the support for them provided by recently developed methods for analyzing calculated electron densities, are reviewed and discussed in this *tutorial review*.

1. Introduction

Although we can obtain very detailed knowledge about the geometry of a molecule from experiment or from *ab initio* calculations, this information does not answer the question "What factors determine the geometry of molecules?" Although we could answer that the observed geometry is that which has a lower energy than any other geometry, this is not satisfactory for most chemists who are looking for a more conceptual and descriptive, if qualitative, answer. Several models have been developed to provide such insight. These models attempt to answer the question "What determines the arrangement of the bonds around any given atom in a molecule?" The simplest type of molecules that we can consider in discussing this question are AX_n molecules, where A is a central atom and X is a ligand atom, and where the A–X bonds may be single, double or triple. Among these models, the valence shell electron pair repulsion (VSEPR) model has become widely accepted for discussing the geometry of molecules of the nonmetals, and it is used extensively, particularly for teaching at the introductory level. The success of the VSEPR model is largely due, as we will discuss, to its recognition of the importance of lone pairs in determining geometry.

Ligand–ligand repulsions, particularly between large bulky groups, have long been considered to be of importance, for example, in determining the rates of S_N2 substitution at a saturated carbon atom. But the importance of such repulsions, between even monatomic ligands, bonded to the same central atom (geminal ligands), in determining the ground state geometry of a molecule has not been generally recognized until quite recently, even though the importance of such repulsions was clearly demonstrated as early as the 1960's for molecules with a central carbon atom. However, a model in which molecular geometry is considered to be determined only by ligand repulsions gives incorrect predictions for molecules in which there are lone pairs in the valence shell of the central atom. Relatively recently though, the ligand–ligand repulsion model has been revived and studied in some detail for other central atoms, including those with valence shell lone pairs. This work has led to the development of the ligand close packing (LCP) model. Alongside the VSEPR and LCP models, the valence bond theory has been used for many years in the discussion of molecular geometry.

In this article we review these models, pointing out their various deficiencies and limitations, as well as a combined VSEPR–LCP model that overcomes most of the deficiencies of

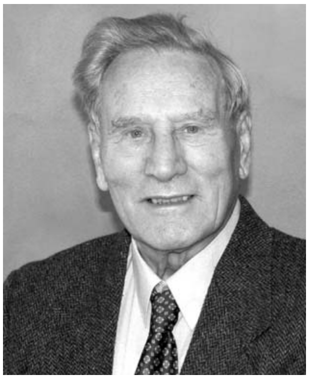

Ronald J. Gillespie

Dr. R. J. Gillespie was born in London and received his B.Sc., Ph.D., and D.Sc. from University College London. He was a lecturer at UCL from 1949 to 1958 when he moved to become Associate Professor and then Professor in the Chemistry Department at McMaster University, Hamilton, Ontario, Canada. His main research interests have been in the chemistry of superacids, fluorine chemistry, noble gas chemistry, and molecular structure and geometry. In 1957 he first proposed the VSEPR model with Prof. R. S. Nyholm and he has continued to develop the model ever since, particularly in recent years.

Edward A. Robinson

Dr. E. A. (Peter) Robinson was born in England and educated at Alleyn's School and University College London. The Robinson–Gillespie connection dates from 1955 at UCL. In Canada in 1958, he became the first member of the Gillespie research team at McMaster University. From 1961 to 1998 he was associated with the University of Toronto as Professor of Chemistry, and from 1966 as a founding member, and sometime Principal and Dean, of the University's Mississauga Campus. He received the D.Sc. Degree from the University of London in 1969.

the separate models and allows reliable qualitative (or even semi-quantitative) predictions of molecular geometry to be made for the vast majority of the molecules of the nonmetals of Groups 13–18. These models have, however, been less successful in accounting for the geometry of many transition metal molecules and we discuss the reason for this and review recent work to develop a model similar to the combined VSEPR–LCP model to account for their geometries.

It is pertinent at this point to mention that the terms 'model' and 'theory' are often used more or less interchangeably. However, we prefer to use the term *theory* to describe a set of rules that are derived from the fundamental laws of nature and the properties of the fundamental particles, such as statistical mechanics and quantum mechanics. In contrast a *model* is a set of empirical rules that give an approximate or qualitative explanation of some particular aspect of a system. Thus VSEPR and LCP are models and not theories. Although in its complete form the valence bond theory can be considered to be a theory, in its commonly used, linear combination of atomic orbitals form it can only be regarded as a model.

2. The VSEPR model

The VSEPR model[1–3] is well known and widely used so that it is not necessary to review it in detail here. Rather we concentrate on its limitations and exceptions to its rules. However, because its physical basis is not always well understood and it is sometimes incorrectly regarded as a purely empirical model, or as an electrostatic model, we also briefly discuss its physical basis.

The VSEPR model assumes that the electron pairs in the valence shell of a central atom, both bonding and non-bonding, keep as far apart as possible. This assumption leads to the well-known AX_nE_m shapes, where E denotes a lone pair. Because electrons are not fixed in space, as implied by Lewis diagrams, but are in constant motion and cannot be precisely located in space, we describe each electron pair in terms of the region of space, called a domain, in which it is most probably to be found. So the basis of the VSEPR model is that the electron pair domains in the valence shell of a central atom adopt the arrangement that keeps them as far apart as possible. An electron pair domain is a qualitative concept that is not precisely defined. But as a simple first approximation a domain can be considered to have a spherical shape as first suggested by Bent in his tangent-sphere model.[4] The geometrical arrangement adopted by a given number of spherical domains in a valence shell is then given by those arrangements in which identical spheres are packed as closely as possible around a central point, or much smaller sphere, representing the core of the central atom as shown in Fig. 1. Recognizing that each domain can be either a bonding domain or a non-bonding domain leads to the familiar $\mathrm{AX_mE_n}$ molecular shapes.

Most molecules exhibit small deviations from the ideal geometries so two rules were introduced in the VSEPR model in order to be able to make predictions about these deviations from the regular polyhedral shapes:

1. Lone pair domains are larger than bonding domains and are not considered to be spherical but to spread around the central core as much as possible so they have a greater angular spread than bonding domains.

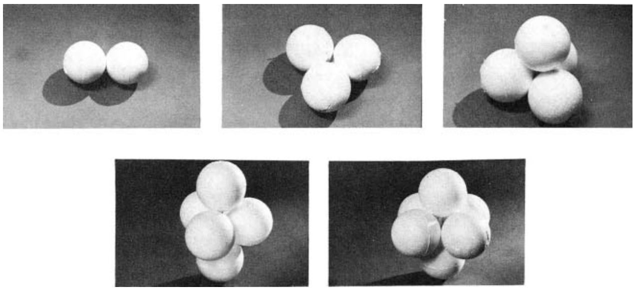

Fig. 1 Sphere models representing the arrangement of two to six electron pair domains in a valence shell surrounding a much smaller core.

2. The size of a bonding domain decreases with increasing electronegativity of the ligand or decreasing electronegativity of the central atom.

These rules are very successful in predicting deviations from regular polyhedral shapes for many molecules, nevertheless, some important exceptions to the VSEPR model still remain.

In order to understand these exceptions we need to discuss the fundamental basis of the VSEPR model which explains why electrons in molecules are found in pairs as first proposed by Lewis; although he had no idea why electrons are found in pairs, he realized that this was apparently inconsistent with Coulomb's law.

2.1 The fundamental basis of the VSEPR model

Even though the physical basis of the VSEPR model was discussed in the original paper on VSEPR,[1] this discussion is often ignored and the tendency for electron pairs to keep as far apart as possible is sometimes considered just as an empirical rule, or erroneously attributed to electrostatic repulsion.

The Pauli principle places a restriction on the form of the wave function for a system of electrons, or any other particle with a half-integral spin (collectively known as fermions); the consequence is that electrons with the same spin have a low probability of being found close together and a high probability of being found far apart, while electrons of opposite spin have no such restriction placed on their motion. In effect, electrons of opposite spin do not "see" each other; they may be found even at the same point in space as far as the Pauli principle is concerned. This was clearly pointed out by Lennard-Jones[5] who stated in 1954 that "*This effect is much more powerful than that of electrostatic force. It does more to determine the shapes of molecules than any other single factor. Its all pervading influence does not seem to have been fully realized by chemists, but it is safe to say that ultimately it will be regarded as the most important property to be learned by those concerned by molecular structure.*"

In a valence shell octet there are 4 α spin and 4 β spin electrons. The four α spin electrons have a most probable arrangement that keeps them as far apart as possible, namely at the vertices of a tetrahedron. Similarly the 4 β spin electrons have a most probable arrangement at the vertices of a tetrahedron that is independent of the α spin tetrahedron

(Fig. 2). In a free atom or ion such as Ne, F^- or O^{2-} the two tetrahedra have no fixed orientation in space and no correlation with each other so that there are no localized pairs and the overall electron density of the valence shell is spherical. However, if for example, an oxide ion is perturbed by the close presence of two nuclei, such as two protons to form an H_2O molecule, electrons are attracted to each of these nuclei. But, as only two electrons of opposite spin can be attracted close to each other, each combining nucleus attracts a pair of opposite spin electrons bringing the two tetrahedra into approximate coincidence with the formation of four $\alpha\beta$ pairs, two bonding and two non-bonding pairs, with an overall tetrahedral arrangement, as proposed by the VSEPR model. The formation of four localized pairs, however, depends on the strength of the attractive force which in turn depends on the relative electronegativities of the ligand and the central atom. When the electronegativity of the ligand is not comparable to or greater than the electronegativity of the central atom the valence shell electrons are not strongly localized into pairs which is one reason for exceptions to the VSEPR model. Another reason is that ligand–ligand repulsions may also be of importance.

3. Ligand–ligand repulsions and the ligand close packing model

Ligand–ligand repulsions are another manifestation of the operation of the Pauli principle which is why atoms with closed-shells resist overlapping each other. There is a repulsion between any closed-shell non-bonded atoms that increases in magnitude with decreasing distance apart. Although these interligand repulsions were not considered in the VSEPR model they are nevertheless an important factor in determining molecular geometry.

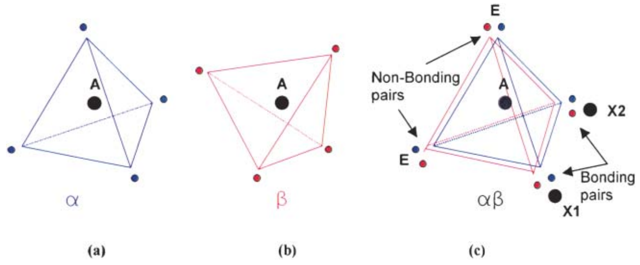

Fig. 2 The Pauli principle and the formation of localized electron pairs in a molecule. (a) The most probable arrangement of four α spin electrons in the valence shell of an atom is that which keeps them as far apart as possible, that is at the corners of a tetrahedron. (b) Similarly, the most probable arrangement of four β spin electrons is at the corner of a tetrahedron, but these two tetrahedral arrangements have no correlation with each other so in a free atom they produce a spherical electron density. (c) The interaction of two ligand cores, such as two protons, draws opposite spin electrons together, forming two bonding and two non-bonding pairs.

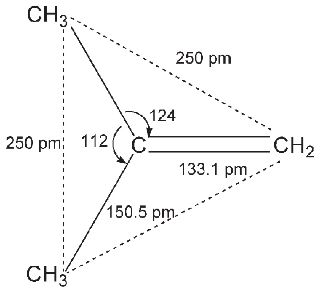

Fig. 3 The structure of 2-methyl propene as determined by Bartell and Bonham[6].

When, in 1960, Bartell and Bonham[6] found that the non-bonding distances between the three carbon atoms surrounding the central carbon in isobutene (2-methyl propene) $(CH_3)_2C{=}CH_2$ are all the same (Fig. 3), they proposed that these three atoms are close packed and that this is the most important factor determining the geometry of this molecule. When ligands are sufficiently close to each other that the repulsive force between them is very strong, and is increasing so steeply with decreasing interligand distance that further overlap of their valence shells is effectively impossible, the ligands can be regarded as hard, approximately spherical, objects that cannot interpenetrate. The carbon atoms in isobutene can therefore be assigned a fixed radius of 125 pm, equal to half the distance between any two carbon ligands. Subsequently, Bartell[7] found that ligand–ligand distances in other three- and four-coordinated molecules with a central carbon atom are also very nearly constant. So he assigned a characteristic radius to each of these ligands such that the sum of two ligand radii gave the distance between any two given ligands (Table 1). However Bartell's proposal that bond angles were determined by ligand packing was contrary to the accepted convention at the time, that molecular geometry and bond angles were a consequence of orbital hybridization, so it was not widely accepted.

Later, other investigators, such as Glidewell[8] attempted to apply Bartell's radii (which have sometimes been referred to as 1,3 radii) to molecules with central atoms other than carbon, but they found that they did not give good predictions of interligand distances. As a consequence, Bartell's model was largely forgotten. Nevertheless, several authors, including Hargittai in particular, continued to claim that ligand–ligand repulsions could be of importance in determining molecular geometry. For example, in his study of the geometry of the SO_2 group in a variety of $XYSO_2$ molecules he noted that, "*The oxygen–oxygen distance is strikingly constant at about 248–249 pm.*" He went on to conclude, "*The constancy of the oxygen–oxygen distance of the SO_2 group indicates that non-bonded atom–atom interactions may be at least as important in determining the geometry of the sulfone group as the electron pair repulsions considered in the VSEPR model.*"[9]

In 1997 Gillespie and Robinson found exactly the same constancy of interligand distances in a large number molecules with other central atoms such as Be, B and N, as Bartell had found for molecules with a central carbon atom (Table 1).[10,11] From these interligand distances, the ligand radii in Table 2 were deduced.[10,11] They called this extension of Bartell's ideas the ligand close packing (LCP) model.[11–13] Ligand radii decrease across the periodic table with increasing electronegativity of the central atom and therefore with decreasing ligand charge. This expected decrease in charge is confirmed by the

Table 1 Interligand distances (pm) for molecules of the Period 2 elements; number of structures considered in italics

	Boron			Central atom Carbon			Nitrogen		
				Interligand distance (X---X)					
H---H	204(2)	*11*		178(2)	*19*		164(2)	*13*	
C---C	274(1)	*5*		252(2)	*19*		240(1)	*6*	
N---N	248(1)	*8*		240(2)	*4*				
O---O	238(2)	*14*		224(2)	*9*		218(2)	*7*	
F---F	226(1)	*23*		216(2)	*34*		214(2)	*3*	
Cl---Cl	302(2)	*17*		290(2)	*16*		(282)		
				Interligand distance (X---Y)					
	Observed		Radius sum	Observed		Radius sum	Observed		Radius sum
H---C				219(1)	*15*	215			
H---N	226	*1*	226						
H---O				203(2)	*6*	201			
H---F	216	*1*	215	204(2)	*7*	197	189(2)	*1*	189
H---Cl				236(2)	*5*	234	222(1)	*1*	222
C---F				234(2)	*8*	234			
C---Cl				271(2)	*7*	271			
N---F	226	*1*	227				240(2)	*4*	
O---N				228(1)	*8*	232			
O---F	232(2)	*7*	232	223(2)	*13*	220			
O---Cl				260(1)	*5*	257			
F---Cl				253(1)	*5*	253	248(3)	*2*	247

Table 2 Ligand radii (pm)[a]

	Central atom				
Ligand	Be	B	C[b]		N
H		102	89		82
C		137	126	*(125)*	120
N	144	124	120	*(114)*	
O	133	119	112	*(113)*	109
F	126	113	108	*(108)*	107
Cl	168	151	145	*(144)*	141

[a] Probable reliability ±2 pm. [b] Bartell radii in italics.

ligand charges calculated as described in Section 7 (Table 3). Fig. 4 shows how the fluorine ligand radii vary with ligand charge for molecules of Period 2. This variation of ligand radius with charge is the main reason why Bartell's concept of ligand close packing fell into disfavour. It was not appreciated that the ligand radius varies with ligand charge and that the Bartell radii would not, therefore, be expected to apply to central atoms other than carbon as Glidewell and others had assumed.

The ligand radii given in Table 2 are independent of the coordination number of the central atom, which for these molecules may be either three or four. For example, the F---F distance of 226 pm is the same in both BF_4^- and BF_3. Thus the substantial difference in the length of the B–F bond in these molecules (Fig. 5) can be simply accounted for by the change in coordination number, in other words, three ligands pack more closely around the central atom than four. There is no reason, therefore, to assume that the observed bond length difference is due to π back-bonding from fluorine to boron giving the B–F bond some double bond character as has often been suggested[14] but for which there is no other evidence (Fig. 5). Moreover, it seems unreasonable to expect that there can be any substantial donation of electron density, whether this be σ or π donation, from the very strongly electronegative fluorine atom to the much more weakly electronegative boron

Table 3 Atoms in molecules (AIM) ligand charges

	Ligand		
	F	Cl	H
LiX	−0.92	−0.91	−0.91
BeX_2	−0.88	−0.84	−0.87
BX_3	−0.81	−0.64	−0.70
CX_4	−0.61	−0.09	−0.04
NX_3	−0.28	+0.08	+0.35
OX_2	−0.13	+0.23	+0.63
FX	0	+0.38	+0.78
AlF_6^{3-}	−0.93		
SiF_6^{2-}	−0.88		
SF_6	−0.76		

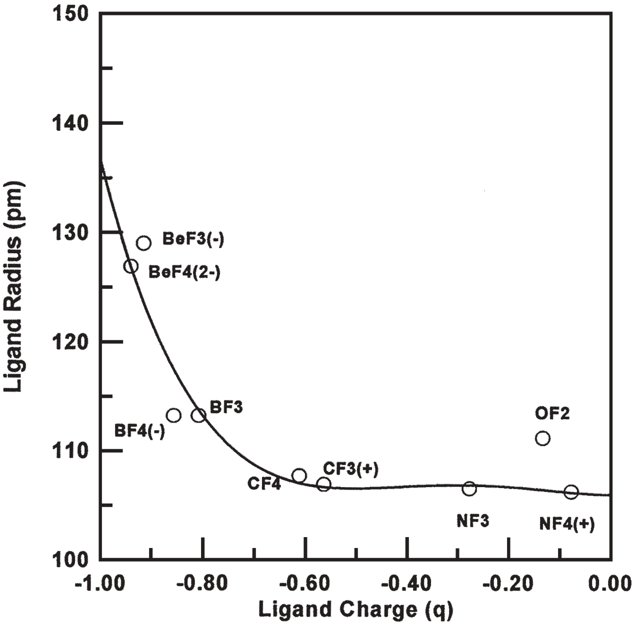

Fig. 4 Plot of the fluorine ligand radius for Period 2 nonmetals against the calculated ligand charge.

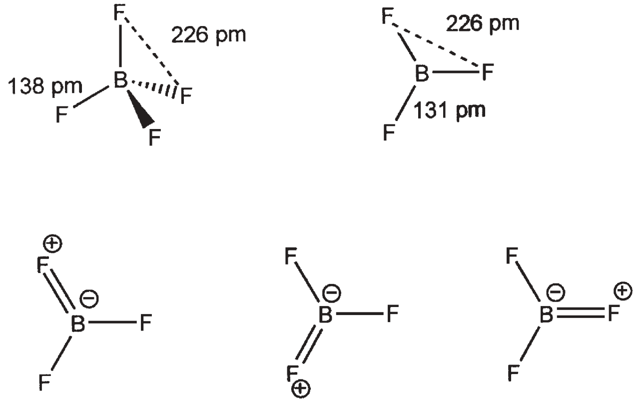

Fig. 5 The structures of BF_3 and BF_4^- and the π back-bonding model of the bonding in BF_3.

atom. Although it is very often assumed that an unexpectedly short bond implies an increased bond order, this is not necessarily so, because both coordination number and bond polarity can also affect bond lengths. Both decreasing coordination number and increasing polarity cause bond lengths to decrease.

It is not only the 3- and 4-coordinated molecules of Be, B and C that are close-packed but also those NX_3E and OX_2E_2 molecules that have strongly localized lone pairs. In these molecules both the ligands and the non-bonding electron pairs may be considered to be close packed. Lone pairs cannot, of course, be assigned a ligand radius. Because they are attracted only by the core of the central atom, they spread out as much as possible around this central core pushing the ligands together until they "touch" that is until the X---X distance is equal to the sum of the X radii, leaving the rest of the space in the central atom valence shell of NF_3 occupied by the lone pair. For example, in NF_3 the F---F distance is 212 pm the same as in NF_4^+ showing that the F ligands are close packed in both molecules.

4. Comparison of the VSEPR and LCP models

We have seen that, at least for Period 2 molecules, ligand–ligand repulsions play an important role in determining molecular geometry. In some cases bond angles can be explained by either ligand–ligand repulsion or the electronegativity of the ligand, but in other cases bond angles can only be explained by ligand–ligand repulsion. For example, the increase in bond angle from NF_3 (102.3°) to NCl_3 (106.8°) can be explained by both models because the ligand electronegativity decreases with ligand size in this series. In contrast, we can only explain the smaller bond angle in PH_3 (93.4°) than in PF_3 (97.8°) by the small size (ligand-radius) of the H ligand, because hydrogen has a much smaller electronegativity than fluorine. The ligand radius of hydrogen in PH_3, obtained from its calculated charge (Section 7), gives a bond angle of 88° which is a little smaller than the observed angle of 93.2°, so that even the small hydrogen ligands are almost close packed because of the large repulsion exerted by the lone pair, emphasizing once again the important influence that lone pairs have on bond angles.[15] We conclude that ligand–ligand repulsion is a better predictor of bond angles than the VSEPR rule concerning the effect of electronegativity on bond angles.

The concept of ligand close packing enables bond angles to be calculated if bond lengths are known. For example, in the series F_2O, FOH, and H_2O whereas the VSEPR electronegativity rule would lead one to expect that the FOH bond angle would be an approximate average of the F_2O (103.1°) and H_2O (104.5°) angles, it is considerably smaller than either of these two angles (Fig. 6). This small angle can, however, be understood in terms of close-packing, as it can be calculated from the F and H ligand radii and the bond lengths to be 99.5°, which is smaller than the angles in both F_2O and H_2O and is close to the observed angle of 97.2°, showing again that the LCP model gives a better explanation of the bond angle than the VSEPR model.

The VSEPR model predicts that the bond angles in AX_3E and AX_2E_2 molecules should be smaller than the regular tetrahedral angle of 109.5°. Although this is generally true, some molecules such as Cl_2O (110.9°), Me_2O (111.7°) and NMe_3 (110.9°) have bond angles slightly greater than 109.5° and a few, such as $(SiH_3)_2O$ (144.1°) and $N(SiH_3)_3$ (120°) have much larger bond angles (Fig. 6). The extent to which these angles are greater than 109.5° depends on the relative importance of two effects: (1) the degree of localization of the valence electrons into pairs, which depends on the difference in electronegativity of the ligand and the central atom, and (2) ligand–ligand repulsions, which depend on the size of the ligands. For Cl_2O, Me_2O, and NMe_3 the difference in electronegativity is not large, so that the valence shell electrons are relatively well localized, and the ligands (C and Cl) are relatively small, so the bond angles are not much larger than 109.5°. In contrast, for $(SiH_3)_2O$ and $(SiH_3)_3N$ the electronegativity of Si is much smaller than that of N or O so the valence shell electrons are only poorly localized, while the ligand Si is much larger than either N or O so that ligand–ligand repulsions are more important and dominate the geometry giving the large observed bond angles. So we may describe $(SiH_3)_2O$ as a predominately ionic molecule, consisting of a central oxygen atom that is close to an O^{2-} ion with only weakly localized electron pairs and two rather positive SiH_3 groups repelling each other, to give the observed large bond angle. The charges calculated as described in Section 7 are O (−1.72) and SiH_3 (+0.86). The large ionic character of the Si–O bonds is responsible for their short length of 163.4 pm (sum of the covalent radii = 183 pm) (Fig. 7). This description is in marked contrast to an earlier, but unlikely, explanation that is still often given in which the large bond angle, and the short Si–O bonds, are accounted for in terms of the donation of lone pair electrons from the very electronegative oxygen atom to the much less electronegative silicon atom giving double bond character to the Si–O bonds.[14] There is, however,

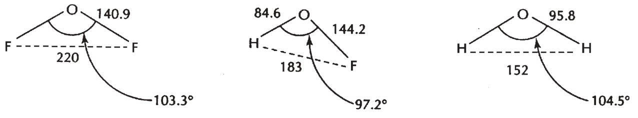

Fig. 6 The structures of F_2O, FOH, and H_2O.

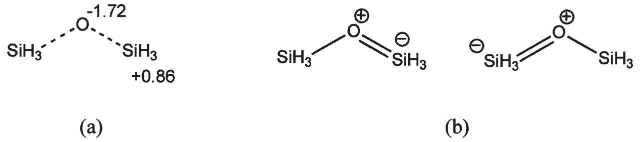

Fig. 7 Two models of the bonding in $(SiH_3)_2O$; (a) the predominately ionic model; (b) the π back-bonding model as described by two resonance structures.

no independent evidence for this double bond character and, as long ago as 1980, it was shown that it is not supported by *ab initio* calculations.[16] The $(SiH_3)_3N$ molecule can be described in a similar way. Thus the apparent deviation of the geometries of some AX_3E and AX_2E_2 molecules from the VSEPR model is not so much a failure of the VSEPR model, but rather a consequence of the fact that the VSEPR model cannot be expected to apply when the ligands are substantially less electronegative than the central atom.

In summary we can say that the two important effects determining bond angles are the extent of localization of the valence shell electrons into opposite spin pairs and ligand–ligand repulsion.

5. Molecules of the elements of Period 3 and beyond

The question naturally arises as to whether the ligands in molecules of the larger elements of Period 3 and beyond are similarly close packed. It has been shown that only in six-coordinated molecules of the Period 3 nonmetals are the ligands close-packed.[17] With the exception of PCl_6^- and a few molecules of the type PF_4(bidentate ligand), the known molecules of this type all contain at least five F atoms so the F ligand radius has been established with some certainty from the data for AF_6 and AXF_5 molecules (Table 4). Less-certain values for the ligand radius of Cl obtained from the data PCl_6^- and SF_5Cl are also included in Table 4. The Period 3 fluorine ligand radii are plotted against the ligand charge in Fig. 8. The six-coordinated fluorides fall on the same smooth curve as for the Period 2 fluorides, confirming that the ligands in these Period 3 molecules are indeed close-packed. In contrast the points for the 3 and 4-coordinated fluorides of the Period 3 elements in Fig. 8 do not fall on this curve, confirming that they are indeed not close packed. Ligand–ligand repulsions must also play a role in determining the geometry of these and other molecules in which the ligands are not close packed. The relative importance of ligand-repulsion and electron pair localization (VSEPR model) is difficult to assess in such cases.

Table 4 Fluorine and chlorine ligand radii (pm) for the Period 3 nonmetals

	Central atom			
	Si	P	S	Cl
F	119	112	111	110
Cl		151	149	

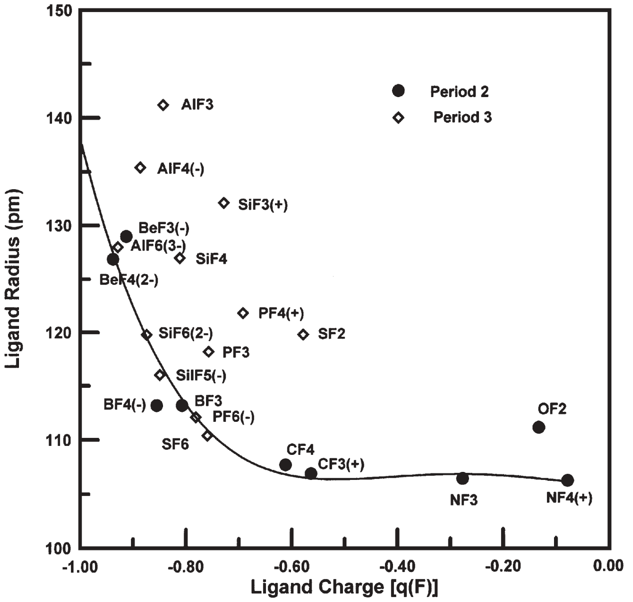

Fig. 8 Plot of the fluorine ligand radius for the Period 2 and Period 3 nonmetals against the calculated ligand charge.

5.1 Five-coordination

Five-coordinated molecules have a number of interesting features that are due to the non-equivalence of the equatorial and axial sites.[17] That the axial sites are more crowded than the equatorial sites means:

1) Axial bonds are longer than the equatorial bonds.
2) Lone pairs occupy the less crowded equatorial sites.
3) Larger ligands occupy the less crowded equatorial sites.
4) Angles involving larger ligands and lone pairs are larger than the regular polyhedral angles.

The geometry of trigonal bipyramidal molecules consistently obeys rules 1–4, as shown by the examples given in Fig. 9, except for one notable exception. In the molecules PHF_4, PH_2F_3, and PH_3F_2, the smaller H ligands unexpectedly occupy the less crowded equatorial sites.[18] However, the deviations from a regular trigonal bipyramidal geometry are consistent with the small size of the hydrogen ligand in that the axial P–F bonds are bent towards the equatorial H ligands, in other words the HPF_{ax} angles are smaller than 90° (Fig. 10). These interesting structures merit further study. Calculations of the structures of related, but unknown, molecules such as $SiH_{5-x}F_x^-$ and $SH_{5-x}F_x$ could well be useful.

5.2 Seven-coordination

The maximum coordination number of the Period 3 elements of Groups 13–18 is six. It is also six for the larger atoms of Period 4, but for the still larger atoms of Period 5 seven- and eight-coordination becomes possible.[2,3,17] Seven-coordination is of particular interest, because, like five-coordination, it is not possible for all the coordination sites to be equivalent. Consideration of ligand–ligand repulsion leads to the conclusion that for an AX_7 molecule there are three possible geometries of very similar energy, the capped trigonal prism, the capped octahedron and the pentagonal bipyramid. For the

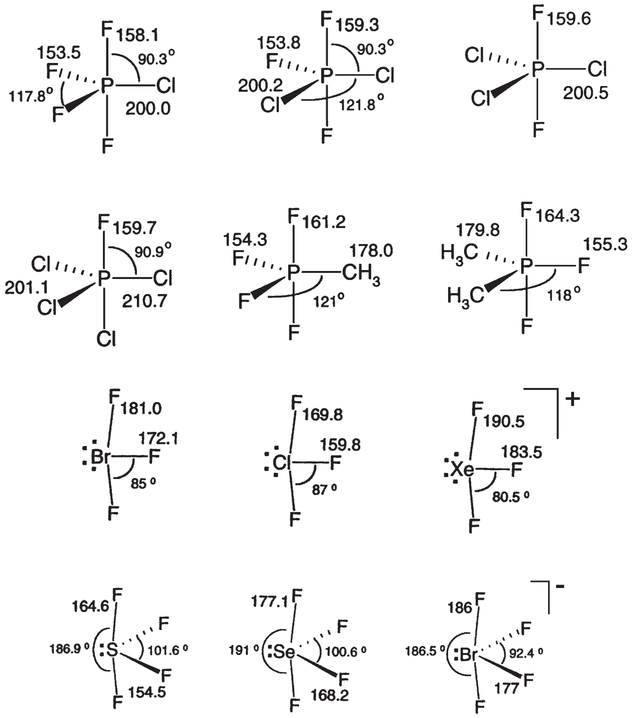

Fig. 9 The structures of some trigonal bipyramidal molecules.

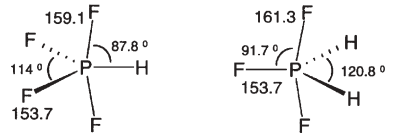

Fig. 10 The structures of two pentavalent phosphorus hydride fluorides.

elements of Groups 13–18 only the pentagonal bipyramid is observed. In this geometry the axial positions are not equivalent to the equatorial positions but, in contrast to the trigonal bipyramid, it is the axial positions that are less crowded than the equatorial positions so that the axial bonds are shorter than the equatorial bonds. Thus larger ligands preferentially occupy the axial sites as shown by the examples in Fig. 11. However, AX_6E molecules have long been recognized as exceptions to VSEPR because they do not have the expected pentagonal pyramidal geometry with one axial lone pair. Rather they have either an undistorted octahedral geometry, for example $SeCl_6^{2-}$, or a C_{3v} distorted octahedral geometry, for example IF_6^- and XeF_6. In these molecules the lone pair has been described as inactive or only weakly active.

In an octahedral molecule AX_6E, such as $SeCl_6^{2-}$, the six chlorine ligands are close packed around the central Se core leaving no room for the lone pair which remains in the spherical outer shell of the core (Fig. 12). Thus the core is effectively Se^{4+} rather than Se^{6+} and is correspondingly larger than an Se^{6+} core so that the Se–Cl bonds are correspondingly unusually long, 241 pm in $SeCl_6^{2-}$ compared with 214 pm in $SeCl_2$ for example. When the ligands are smaller, as in SeF_6^{2-}, they are not quite close packed leaving some room for the non-bonding "lone-pair" electrons, but not enough for them to enter fully into the valence shell to form a fully stereochemically active lone pair to give a pentagonal pyramidal geometry. But they enter the valence shell sufficiently to distort the octahedron so that the FSeF angles surrounding the expected partial lone pair position are larger than 90° and these Se–F bonds are longer than the other three Se–F bonds (Fig. 12). When the central atom is a little smaller, as in BrF_6^-, the ligands are again close packed, there is no space for the lone pair and the molecule has a regular octahedral geometry. Because of the larger size of the Period 5 atoms both IF_6^- and XeF_6 have the C_{3v} distorted octahedral structure (Fig. 13).

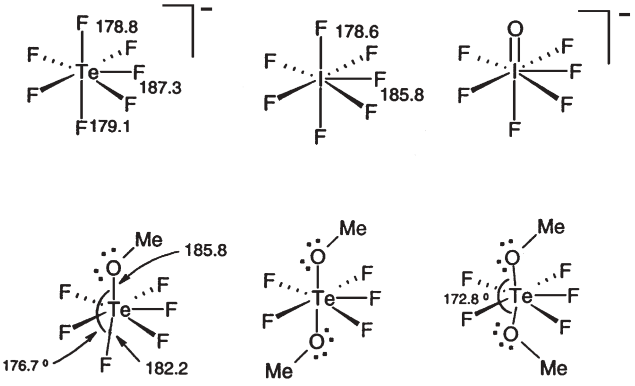

Fig. 11 The structures of the pentagonal bipyramidal AX_7 molecules.

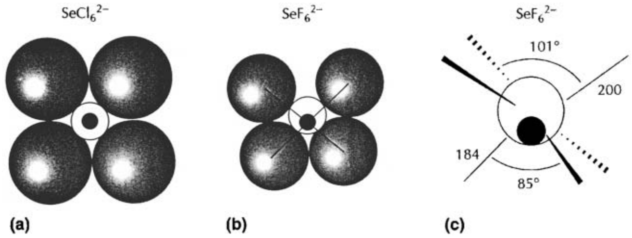

Fig. 12 Close packing models of $SeCl_6^{2-}$ and SeF_6^{2-}.

It is interesting that the unique pentagonal planar XeF_5^- ion has the expected geometry with a lone pair in each of the two axial positions (Fig. 14). If the two non-bonding pairs remained in the core they would give a very ellipsoidal core with most probable positions of the two pairs on opposite sides of the nucleus. It is immaterial whether we describe the molecule as having two lone pairs in the valence shell of the Xe atom or as having an ellipsoidal core, because in both cases the geometry is expected to be pentagonal planar.

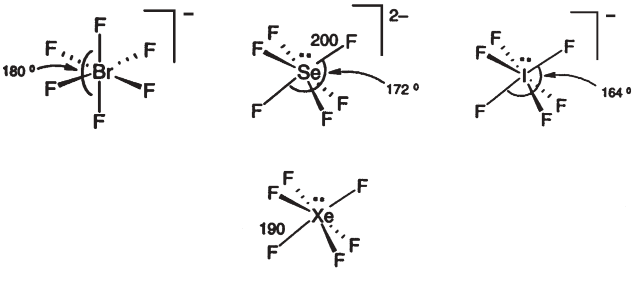

Fig. 13 The structures of some AX_6E molecules.

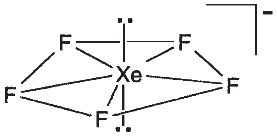

Fig. 14 The pentagonal planar structure of XeF_5^-.

6. The combined VSEPR–LCP model.

Combining ideas from both the LCP and VSEPR models gives a model that can be used to understand the geometry of almost any molecule of the elements in Groups 13 to 18, *i.e.* the molecules of the nonmetals.

The geometry of the ligands surrounding a central atom is determined by two important effects:

(1) The interaction of the ligands with the central atom causes the localization of the valence shell electrons of the central atom into opposite spin pairs that are most probably located as far apart as possible. The extent to which this happens depends on the strength of the interaction between the ligands and the central atom. When the ligands have a comparable or a greater electronegativity than the central atom, as is very often the case, this interaction is strong and causes the valence shell electrons of the central atom to be localized into opposite spin pairs, both bonding and non-bonding, which have a most probable arrangement in which they are as far apart as possible, as a consequence of the operation of the Pauli principle. As we have seen this is the basis of the VSEPR model.

(2) The ligands repel each other which is also a consequence of the Pauli principle.

Both effects operate in all molecules. For molecules in which there are no lone pairs on the central atom, *i.e.* AX_2, AX_3, AX_4, AX_5, AX_6, both the VSEPR model and the ligand–ligand repulsion model predict the same geometries and it is not possible to determine their relative importance. For molecules in which there are well-defined lone pairs in the valence shell of the central atom, the lone pairs dominate the geometry. Many apparent exceptions to the VSEPR model can be attributed to the assumption that the lone pairs of a conventional Lewis structure are in fact present. This may not always be the case for two reasons:

(1) In some molecules the ligands interact only very weakly with the central atom so that only very weakly localized lone pairs are formed, as in the molecules $O(SiH_3)_2$ and $N(SiH_3)_3$.

(2) For molecules in which there are six ligands and a formal lone pair the valence shell is so crowded with ligands that there is sometimes no space available for the non-bonding electrons. In such cases the two non-bonding electrons remain wholly or partly in the core of the central atom.

Even in molecules in which lone pairs dominate the geometry, ligand–ligand repulsions play an important role in that they oppose the effect of lone pairs on bond angles. In molecules in which the ligands are close packed, as is the case for most AX_2E_2 and AX_3E molecules of the elements of Period 2, and the AX_5E molecules of the elements of Period 3, lone pairs decrease bond angles until the ligands "touch", that is until the ligand–ligand distance is equal to the sum of the ligand radii.

The VSEPR model is based on the interactions between bond pairs, between lone pairs and bond pairs, and between lone pairs, while the ligand repulsion model is based on the interactions between ligands, between ligands and lone pairs and between lone pairs. The two models are essentially the same except that ligand repulsions replace bond–bond repulsions. Since the electron density associated with a bond cannot be clearly distinguished from that associated with a ligand there is no obvious way to distinguish between the two models. Moreover, there is no way to measure or quantify the strength of bond–bond repulsions. In contrast, ligand repulsions are determined by the size of the ligand, which in close packed molecules can be measured in terms of the ligand radius. The VSEPR concept of bond–bond repulsion is therefore replaced by that of ligand–ligand repulsion in the combined VSEPR–LCP model.

7. Analysis of the electron density

In recent years there has been considerable interest in the topological analysis of the electron density to provide information on bonding and geometry. This work was pioneered by Bader in his "*Atoms in Molecules*" (AIM) analysis.[19,20,3] It partitions the molecule into its component atoms (atomic basins) by means of zero-flux (interatomic surfaces) that are obtained from the gradient vector field of the density. A simple explanation of the gradient vector field is given in reference 21. Fig. 15 shows a contour map of the electron density of BCl_3 in the plane of the molecule. The interatomic surfaces cut through this plane along the valleys between the peaks (maxima) in the density which occur at the positions of the nuclei. The importance of this partitioning is that it enables any property of a molecule to be separated into its atomic components by integrating the property over each

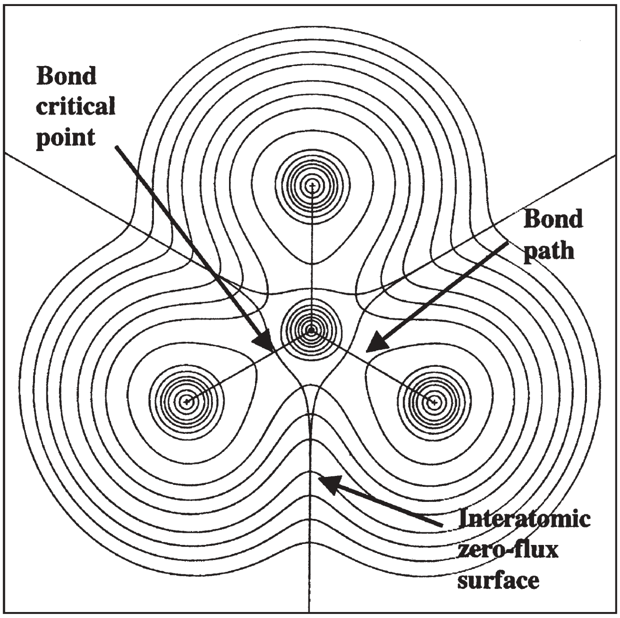

Fig. 15 Plot of the electron density in the plane of the BCl_3 molecule showing the maxima at the nuclei, the interatomic (zero flux) surfaces, and the bond paths.

atomic basin For example the charge associated with each of the ligand atoms can be determined in this way. Between each pair of bonded atoms there is a ridge of electron density that is associated with the bond between the two atoms and is called a bond path. The point of minimum density along this bond path, where the interatomic surface cuts the bond path, is called the bond critical point.

Bader has also pioneered another way of analyzing the density, namely by means of its second differential or Laplacian ($\nabla^2\rho$).[19,20,3] which shows where the electron density in an atom or a molecule is concentrated or depleted. For an atom it shows spherical shells of charge concentration separated by regions of charge depletion corresponding to the conventional electron shells. For a molecule it shows these shells in the core of each atom and also the valence shell, but this shell is not a region of spherical electron density concentration but has a lower symmetry because it has maxima and minima. It is customary to plot $-\nabla^2\rho$ because the maxima in this function show where electron density is locally most concentrated and the minima show where it is most depleted. Except in a very few molecules the number and geometry of these maxima has been found to correspond in number and geometry with the lone pair and bonding domains of the VSEPR model, consistent with the expectation that electron density is concentrated in the bonding and lone pair regions of a molecule.[19–24,3] Fig. 16 shows the isosurfaces (envelopes) for a given value of the Laplacian of the electron density for the NH_3 and PF_3 molecules. These envelopes surround each of the maxima and they correspond well with the electron pair domains of the VSEPR model. Moreover the Laplacian gives us useful information about the extent of localization of the valence shell electrons into non-bonding and bonding pairs. For example, comparison of the Laplacian maps in the plane of the $(CH_3)_2O$ and $(SiH_3)_2O$ molecules (Fig. 17) shows that the electrons in the valence shell of the oxygen atom in $(CH_3)_2O$ are much more localized than in $(SiH_3)_2O$ in accordance with the low electronegativity of the SiH_3 group as we discussed in Section 4.[25]

Another well-known method for analyzing the electron density, known as the electron localization function (ELF)[26–28] shows those regions (called localization basins) where the concentration of opposite-spin pairs is greater than in other regions of a molecule. Again it is found that the number and geometry of the maxima in the ELF correspond to the electron pair domains of the VSEPR model. These maxima are of two kinds: (1) those that share a surface with two atomic cores, called disynaptic, that are formed by the bonding electrons and (2) those that share a surface with only one atomic core, called monosynaptic, that are formed by the lone pair electrons. Fig. 16 shows the isosurfaces corresponding to a given value of the ELF surrounding each of these maxima for the NH_3 and PF_3 molecules, where they may be compared with the Laplacian electron density concentrations. They correspond to the bonding and lone pair electrons of the VSEPR model and thus confirm that the basis of the VSEPR model is the formation of partially localized opposite spin pairs as a consequence of the operation of the Pauli principle.

The ELF permits the number of electrons in each bonding and non-bonding region to be found by integrating the electron density over each corresponding localization basin. In accordance with expectation, the number of electrons in the bonding region of a non-polar covalent bond is close to two, and is less than two for bonds with some ionic character where some of the electron density moves from the bonding region to the non-bonding regions with increasing electronegativity of the more electronegative atom.[29]

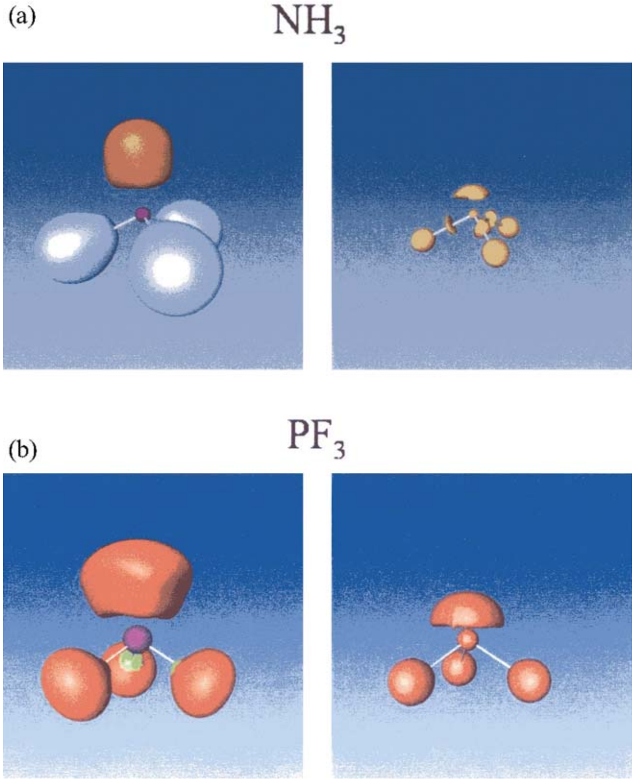

Fig. 16 (a) NH_3: Isosurfaces of the electron localization function (ELF) (left), central core purple, N lone pair brown and H blue. Isosurfaces of the Laplacian (right) of the electron density . (b) PF_3: Isosurfaces of the ELF (left), central core purple, P lone pair brown, bonding electrons green, F non-bonding electrons brown. Non-bonding pairs are not expected and are not observed because of the cylindrical symmetry of the P–F bond.

8. The valence bond (VB) theory

Throughout the preceding discussion there has been no mention of orbitals showing that molecular geometry can be explained and predicted qualitatively without the use of any orbital model. However, the valence bond theory is widely used in the discussion of molecular geometry so we briefly examine its relation to the VSEPR–LCP model. The VB theory is used to describe the bonding in a molecule. In its simplest and commonly used form it assumes that bonds can be described in terms of localized orbitals formed by the overlap of singly occupied atomic or hybrid orbitals on each of the bonded atoms. For example the bond in the H_2 molecule is described by the overlap of two singly occupied 1s orbitals to form a σ bonding orbital containing two electrons. The Pauli principle enters into the VB model by placing the restriction that the maximum number of electrons that can occupy an

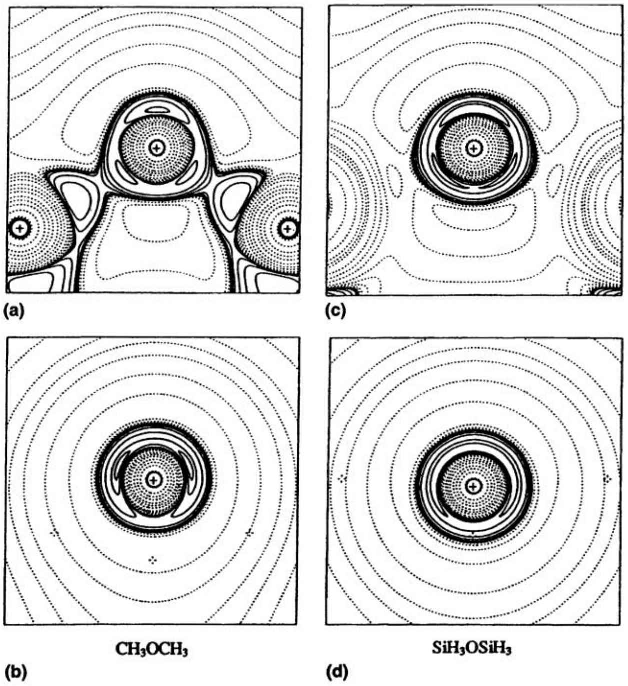

Fig. 17 Plot of the Laplacian of the electron density in the symmetry plane of the molecules $(CH_3)_2O$ and $(SiH_3)_2O$, showing the much smaller localization of the oxygen valence electrons in $(SiH_3)_2O$ than in $(CH_3)_2O$. (a) and (c) are plots in the plane of the molecule and (c) and (d) are plots in the perpendicular plane through the O atom. In (c) the two well-localized electron pairs are seen clearly whereas in (d) the two lone pairs are not resolved and are not at all well localized.

orbital is two and that these electrons must be of opposite spin. Other diatomic molecules such as Cl_2 are described as having a localized Cl–Cl σ bonding orbital and localized non-bonding lone pair orbitals that are associated with only one Cl atom.

The oxygen atom in its ground state has the electron configuration $1s^22s^22p_x{}^22p_y{}^12p_z{}^1$, so each bond in the water molecule is described by a localized bonding orbital formed by the overlap of a singly occupied 2p orbital with the 1s orbital of a hydrogen atom. It is assumed that the bonds are formed in the direction of the maxima of each p orbital as this gives maximum overlap. So this description predicts an angular molecule, but with a 90° rather than the observed 104.5° bond angle. The carbon atom has the ground state configuration $1s^22s^22p_x{}^12p_y{}^1$ with two unpaired electrons available for bond formation. However, four singly occupied orbitals are needed for the formation of four localized bonding orbitals to describe the four bonds in methane and many other molecules of carbon. It is assumed that the formation of the four bonds may be described on the basis of the four singly occupied orbitals in the $1s^22s^12p_x{}^12p_y{}^12p_z{}^1$ excited state of the carbon atom which would give three equivalent bonding orbitals and one non-equivalent bonding orbital. However, in order to describe the four equivalent bonds in the methane molecule, four equivalent orbitals are needed. Because any linear combination of the solutions of the Schrödinger equation for a system is also a solution, the four atomic orbitals can be transformed into four equivalent sp^3 hybrid orbitals pointing in the tetrahedral directions. This transformation is justified on the grounds that these tetrahedral orbitals give a greater overall overlap with the four H 1s orbitals and therefore stronger bonds. This description is clearly consistent with the VSEPR model of four localized electron pair domains with a tetrahedral geometry, but is arrived at by a less direct argument, and it makes the assumption that the four bonds are equivalent although there is no *a priori* reason why this should be the case. The same set of sp^3 hybrid bonds is also used to give a better, but only approximate, description of the bonding in H_2O, F_2O, NH_3, NF_3 and similar molecules, predicting a bond angle of 109.5°. In general these molecules have bond angles that differ from this value and are generally smaller. The VB theory cannot predict these angles which can be predicted qualitatively by the VSEPR model and in many cases quantitatively by the LCP model. Of course the degree of hybridization of the bonding orbitals can be calculated from the observed bond angle but this does not provide a prediction or explanation of the observed bond angle. In general the VB model is much more limited in its ability to predict and explain the geometry of simple molecules than the VSEPR model.

9. Molecular orbital (MO), VB, and VSEPR–LCP models of double bonds

The differences between the MO, VB and VSEPR models are seen clearly in their different descriptions of double bonds. The simple LCAO version of molecular orbital theory cannot be used to describe and predict the geometry of individual bonds and lone pairs and so is not very useful for discussing and predicting molecular geometry. In the much more sophisticated version used in *ab initio* calculations, MO theory can be used to calculate the geometry of a molecule to a good accuracy but it then gives no real understanding of the factors determining the geometry of the molecule.

The terminology of the MO theory is, however, commonly used for the description of multiple bonding. For example each carbon atom in ethene is described as forming three coplanar sp^2 σ bonds, the two C–H bonds and one component of the C=C double bond. The second component of the double bond is assumed to be formed by the "sideways" overlap of the two singly occupied p orbitals on each of the carbon atoms. It is important to note that this is a *description* of the bonding in terms of localized orbitals based on the known geometry of the molecule and it does not *predict* or explain this geometry because the assumption of sp^2 hybridization of the carbon atoms is based on the known planar geometry. In contrast the VSEPR model based on the tetrahedral arrangement of four bonding pairs around each carbon atom does predict the planar geometry, as is often illustrated by simple molecular models using bent springs to denote the two components of the double bond (Fig. 18). Neither of these simple models correctly predicts the observed XCX bond angles which lie between the value of 120° for the σ–π description and the value of 109.5° for the VSEPR model (Table 11). For example, in ethene the HCH bond angle is 117.4° while in C_2F_4 it is only 112.4°. Similarly the VB model based on the tetrahedral geometry of four sp^3 hybrid orbitals on each carbon atom, two on each carbon atom being used to form two bent bonds, gives a very

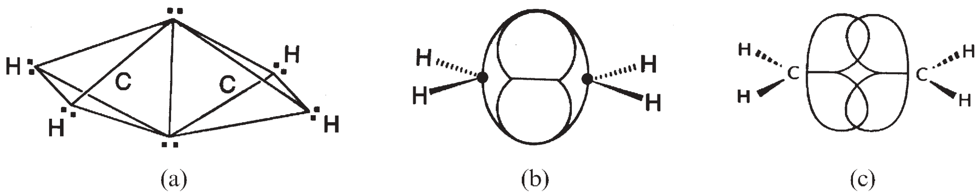

Fig. 18 The VSEPR and VB models of ethene. (a) Tetrahedral arrangements of the electron pairs around each carbon atom. (b) Domain model of the double bond. (c) The VB model showing the overlapping pairs of sp^3 orbitals forming the two bent bonds.

similar description of the double bond and also predicts the overall planar geometry of the molecule.

Fig. 19 shows that ethene is one of the few molecules for which the Laplacian and the ELF do not give very similar pictures of the bonding. Whereas the Laplacian shows two maxima along the bond axis which is not the picture that is usually deduced from the σ–π model or the VSEPR model, the picture given by the ELF, which shows two maxima one on each side of the internuclear axis, does correspond to the VSEPR model. Although the positions of maximum electron concentration given by the Laplacian of the density very frequently have the same number and angular distribution around the core as the ELF localization basins, it is not surprising, in view of their different definitions, that this is not always the case, and shows that the position of maximum concentration of electron density does not always correspond with the position of maximum localization of electron pairs.

10. Molecules of the transition and Group 2 metals

It has long been known that many transition metal molecules do not have the geometry predicted by either the VSEPR or ligand–repulsion models. An important difference between these molecules and those of the nonmetals is that there are no lone pairs in the valence shell of the metal atom so that both these models would lead to the same prediction. The observed deviations from the expected geometries have been explained by the crystal and ligand field models as being due to the interaction of the d electrons in the core, with the ligands. However, there are many transition metal molecules, as well as molecules of the Group 2 elements, that, formally at least, have no d electrons in the core. These molecules, often called d^0 molecules, are therefore expected to have ns^2np^6 spherical cores and to have geometries in accordance with the VSEPR and ligand repulsion models. However, although many d^0 molecules do have the expected geometry, many do not. The various theories and models that have been proposed to attempt to explain these geometries have been very thoroughly and extensively reviewed by Kaupp[30] so they are not discussed here. Instead we review some recent work on the Period 4 metal fluorides, hydrides and methanides, that is not based on the orbital models discussed by Kaupp but on the analysis of the electron density by means of the Laplacian and the ELF. These functions provide the basis for a model for molecules of the metals that is along the lines of the VSEPR–LCP model. This work has shown that the outer shell of the metal atom core, the M shell for the Period 4 molecules, does in fact contain d electron density and is accordingly not spherical but has local concentrations of charge in the Laplacian analysis[31,32] or electron localization basins in the ELF analysis.[33] The Laplacian charge concentrations and the ELF localization basins are identical in number and geometry in all the molecules studied so far. For convenience we call them core domains. They are formed by the interaction of the ligands with the M shell electrons which localizes opposite spin pairs opposite each ligand (ligand opposed core basins) and by electron–electron interaction within this shell in a similar way to the formation of lone pairs and bonding pairs in the valence shell of a nonmetal atom in a molecule. Ligands tend to avoid these core domains and seek regions of diminished electron pair localization or electron density depletion, just as they avoid lone pairs in molecules of the nonmetals. Thus the core domains affect the geometry of the molecule in much the same way as lone pairs affect the geometry of a nonmetal molecule so that the geometry is not always that predicted by ligand–ligand repulsions. For example CaH_2, for which ligand–ligand repulsion would predict a linear geometry, has a bent geometry with a bond angle of 157°. The ELF of the Ca core has four core domains with a C_{2v} distorted tetrahedral (disphenoidal) arrangement in which the ligands face two of the faces of the disphenoid formed by the core domains so the molecule is angular not linear (Fig. 20).[24,31] Two of the core basins are formed by the repulsion between the ligands and the M shell electrons (ligand opposed core basins) and so are situated on the opposite side of the inner core opposite each of the two ligands. The other two are formed by Pauli repulsion between the electrons in these core basins and the other M shell electrons. The large bond angle shows the importance of ligand–ligand repulsions in determining the geometry of this molecule. In the absence of any ligand–ligand repulsions the

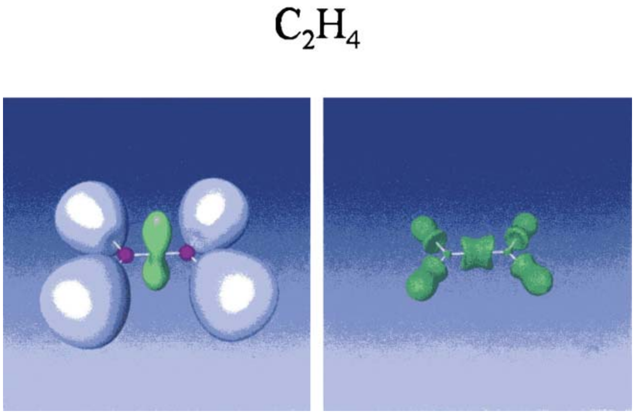

Fig. 19 Ethene: isosurfaces of the ELF (left), cores purple, bonding electrons green, and H blue. Isosurfaces of the Laplacian of the electron density (right).

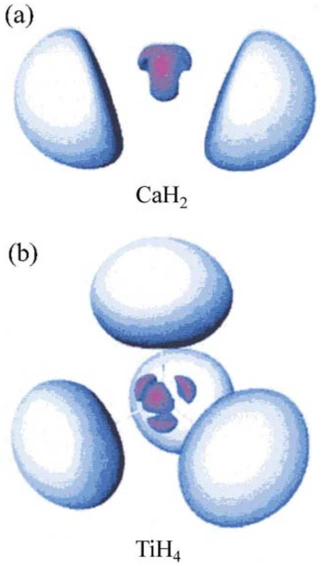

Fig. 20 Isosurfaces of the ELF for (a) $Ca(CH_3)_2$, showing the four core localization basins with a disphenoidal geometry and the two ligands situated opposite two of the faces of the disphenoid; (b) $Ti(CH_3)_4$, showing the four core localization basins with a tetrahedral geometry and the four ligands opposite each of the four faces of the tetrahedron.

core basin would be expected to have a tetrahedral geometry giving a bond angle of 109.5°. In contrast in TiH_4, which has the tetrahedral geometry expected on the basis of ligand–ligand repulsion, the four core domains formed opposite each of the ligands have a reciprocal tetrahedral geometry with the ligands facing each of the faces of the tetrahedron of core basins and thus in the positions of minimum interaction with the core domains. So in this case the interaction between the ligands and the core basins reinforces the tetrahedral geometry predicted by ligand–ligand repulsion.[31] The geometry of the d^0 fluorides, hydrides and methanides of the Period 4 metals, from Ca to Cr, and the dioxides of Ti, V, Cr and Mn has been discussed in detail in reference 32. This work not only gives a convincing explanation of the geometries of these d^0 molecules but it also forms the basis for future studies along the same lines on other d^0 molecules, such as those discussed recently by McGrady and Downs,[33] as well as of d^1 to d^9 transition metal molecules.

Ronald J. Gillespie and Edward A. Robinson
Dept. of Chemistry, McMaster University, Hamilton, Ontario, Canada. E-mail: ronald.gillespie@sympatico.ca

References

1 R. J. Gillespie and R. S. Nyholm, *Q. Rev. Chem. Soc.*, 1957, **61**, 339.
2 R. J. Gillespie and E. A. Robinson, *Angew Chem, Int. Ed. Engl.*, 1996, **35**, 495.
3 R. J. Gillespie and P. L. A. Popelier, *Chemical Bonding and Molecular Geometry*, Oxford University Press, New York and Oxford, 2001.
4 H. A. Bent, *J. Chem. Educ.*, 1963, **40**, 446–523; H. A. Bent, *J. Chem. Educ.*, 1968, **45**, 768.
5 J. E. Lennard-Jones, *Adv. Sci.*, 1954, **11**, 136.
6 L. S. Bartell and R. S. Bonham, *J. Chem. Phys.*, 1960, **32**, 624.
7 L. S. Bartell, *J. Chem. Phys.*, 1960, **32**, 627.
8 C. Glidewell, *Inorg. Chim. Acta.*, 1975, **12**, 219; C. Glidewell, *Inorg. Chim. Acta.*, 1976, **20**, 113.
9 I. Hargittai, *The Structure of Volatile Sulfur Compounds*, D. Reidel Pub. Co, Dordrecht, Holland, 1985, p. 215.
10 E. A. Robinson, S. A. Johnson, T.-H. Tang and R. J. Gillespie, *Inorg. Chem.*, 1997, **36**, 2022.
11 R. J. Gillespie and E. A. Robinson, *Adv. Mol. Struct. Res.*, 1998, **4**, 1.
12 R. J. Gillespie, G. L. Heard and E. A. Robinson, *J Mol. Struct.*, 1999, **485**, 305.
13 R. J. Gillespie, *Coord. Chem. Rev.*, 2000, **51**, 197.
14 C. E. Housecroft and A. G. Sharpe, *Inorganic Chemistry*, Prentice Hall, 2001, pp. 267 and 294.
15 E. A. Robinson and R. J. Gillespie, *Inorg. Chem.*, 2004, **43**, 2318.
16 H. Oberhammer and J. E. Boggs, *J. Am. Chem. Soc.*, 1980, **102**, 7241.
17 E. A. Robinson and R. J. Gillespie, *Inorg. Chem.*, 2003, **42**, 3865.
18 D. Christen, K. Karle, A. Lietke, R. Miskewitze and H. J. Oberhammer, *J. Phys. Chem.*, 1989, **93**, 6672; A. G. Downs, G. S. McGrady, E. A. Barnfield and D. W. H. Rankin, *J. Chem. Soc., Dalton Trans.*, 1989, 645.
19 R. F. W. Bader, *Atoms in Molecules: A Quantum Theory*, Oxford University Press, Oxford, 1990.
20 P. L. A. Popelier, *Atoms in Molecules: An Introduction*, Prentice Hall, Harlow, UK, 2000.
21 C. F. Matta and R. J. Gillespie, *J. Chem. Educ.*, 2002, **79**, 1141.
22 R. F. W. Bader, R. J. Gillespie and P. J. MacDougall, *J. Am. Chem. Soc.*, 1988, **110**, 7329.
23 R. J. Gillespie, I. Bytheway, R. S. DeWitte and R. F. W. Bader, *Inorg. Chem.*, 1994, **33**, 2115.
24 I. Bytheway, R. J. Gillespie, T.-H. Tang and R. F. W. Bader, *Inorg. Chem.*, 1995, **34**, 2407.
25 R. J. Gillespie and S. A. Johnson, *Inorg. Chem.*, 1997, **36**, 3031.
26 A. D. Becke and K. E. Edgecombe, *J. Chem. Phys.*, 1990, **92**, 1960.
27 B. Silvi, *Actual. Chim.*, March 2001, 15.
28 A. Savin, O. Jepson, J. Flad, O. K. Anderson, H. Preuss and H. G. von Schnering, *Angew. Chem., Int. Ed. Engl.*, 1992, **31**, 187.
29 S. Noury, B. Silvi and R. J. Gillespie, *Inorg. Chem.*, 2002, **41**, 2164.
30 M. Kaupp, *Angew. Chem. Int. Ed.*, 2001, **40**, 3534.
31 R. J. Gillespie, I. Bytheway, T.-H. Tang and R. F. W. Bader, *Inorg. Chem.*, 1996, **35**, 3954.
32 R. J. Gillespie, S. Noury, J. Pilmé and B. Silvi, *Inorg. Chem.*, 2004, **43**, 3248.
33 G. S. McGrady and A. J. Downs, *Coord. Chem. Rev.*, 2000, **197**, 95.